We are IntechOpen, the world's leading publisher of Open Access books Built by scientists, for scientists

4,800
Open access books available

122,000
International authors and editors

135M
Downloads

Our authors are among the

154
Countries delivered to

TOP 1%
most cited scientists

12.2%
Contributors from top 500 universities

CLARIVATE ANALYTICS BOOK CITATION INDEX INDEXED

WEB OF SCIENCE™

Selection of our books indexed in the Book Citation Index in Web of Science™ Core Collection (BKCI)

Interested in publishing with us?
Contact book.department@intechopen.com

Numbers displayed above are based on latest data collected.
For more information visit www.intechopen.com

Chapter 1

Re-derivation of Young's Equation, Wenzel Equation, and Cassie-Baxter Equation Based on Energy Minimization

Kwangseok Seo, Minyoung Kim and Do Hyun Kim

Additional information is available at the end of the chapter

http://dx.doi.org/10.5772/61066

Abstract

Recently, Young's equation, the Wenzel equation, and the Cassie-Baxter equation have been widely used with active research on superhydrophobic surfaces. However, experiments showed that the Wenzel equation and the Cassie-Baxter equation were not derived correctly. They should be reviewed on a firm physical ground. In this study, these equations are re-derived from a thermodynamic point of view by employing energy minimization and variational approach. The derivations provide a deeper understanding of these equations and the behavior of a contact angle. Also, in applying these equations, the limitations and considerations are discussed. It is expected that this study will provide a theoretical basis for the careful use of these equations on rough or chemically heterogeneous surfaces.

Keywords: Young's equation, Wenzel equation, Cassie-Baxter equation, contact angle, energy minimization, variational method

1. Introduction

The easiest way to determine the wetting property is to drop a liquid drop on the surface. The drop on the surface forms a unique contact angle depending on the wetting property. By measuring the contact angle, it is easy to examine the surface wettability. Young's equation on the ideal surface, the Wenzel equation on the surface with roughness, and the Cassie-Baxter equation on the surface with chemical heterogeneity have been widely used for the analysis of the contact angle. Although these equations were not derived correctly, they have been used without consideration of the limitations. Application of these equations to surfaces such as a

surface with large contact angle hysteresis that do not meet the conditions for these equations can give errors inherently.

In this chapter, Young's equation, the Wenzel equation, and the Cassie-Baxter equation will be re-derived by energy minimization and variational approach. From analyses of the derivations, properties of a contact angle will be reviewed. Also, the limitations and the considerations will be discussed in applying these equations to various surfaces. We expect that this study will help in the understanding of the nature of the contact angle and its application.

1.1. Young's equation, Wenzel equation, and Cassie-Baxter equation

It is possible to quantify the wettability of a surface by simply measuring the contact angle of a drop resting on a surface. Young's equation has been used as a basic model. Application of this equation is limited to an ideal surface that is rigid, perfectly flat, insoluble, non-reactive, and chemically homogenous. The surface is assumed to have no contact angle hysteresis. On the surface, a contact angle of liquid drop can be described by the following Young's equation:

$$\gamma_{sl} + \gamma \cos\theta = \gamma_{so} \tag{1}$$

where γ, γ_{sl}, and γ_{so} are liquid/gas surface tension, solid/liquid interfacial energy, and solid/gas surface energy, respectively. The apparent contact angle (θ) is an equilibrium contact angle (θ_Y). However, since all the real surfaces are not ideal, models were developed to describe the contact angles on the real surfaces.

There are two models to describe the contact angle on a real surface, i.e. the Wenzel model and the Cassie-Baxter model. Contrary to the ideal surface, the real surface can have chemical heterogeneity and surface roughness. The Wenzel model considers the rough surface but with chemical homogeneity [1]. The Cassie-Baxter model considers the flat surface but with chemical heterogeneity [2].

In the Wenzel model, the surface roughness r is defined as the ratio of the actual area to the projected area of the surface. The Wenzel equation can be written as:

$$\cos\theta^* = r \cos\theta_Y \tag{2}$$

where θ^* is the apparent contact angle and θ_Y is the equilibrium contact angle from Young's equation on an ideal solid without roughness.

In the Cassie-Baxter model, f_1 and f_2 are the area fractions of solid and air under a drop on the substrate. The Cassie-Baxter equation can be written as:

$$\cos\theta^* = f_1 \cos\theta_Y - f_2 \tag{3}$$

http://dx.doi.org/10.5772/61066

where θ^* is the apparent contact angle and θ_Y is the equilibrium contact angles on the solid.

From the Wenzel model, it can be deduced that the surface roughness amplifies the wettability of the original surface. Hydrophilic surface becomes more hydrophilic and hydrophobic surface more hydrophobic. In the Cassie-Baxter model, the area fractions under the drop is important in that the larger the area fraction of air, the higher the contact angle. Although these two models were proposed half a century ago, these equations have been widely used recently with active research on superhydrophobic surface [3-6].

1.2. The fallacy of the Wenzel model and the Cassie-Baxter model

In the Wenzel model and the Cassie-Baxter model, the contact angles were obtained from the non-smooth or chemically heterogeneous state of the surface under the drop. However, Gao and McCarthy demonstrated the fallacy of these models experimentally [7]. They prepared a surface with a hydrophilic spot on a hydrophobic surface, as shown in Fig. 1a. Fig. 1b shows a smooth hydrophobic surface with a superhydrophobic spot. D and d are mean diameters of the drop and the spot.

With various diameters of the drops and the spots, advancing and receding contact angles were measured. They proved that the state of internal surface inside the triple line does not affect the contact angles experimentally and the contact angles are determined only by the state of the surface at triple contact line. It means that the previous Wenzel model and Cassie-Baxter model should be revised for rigid physical meaning [7]. Since then, an active discussion on them has been made [8-12]. Also, these models have been derived in a more rigorous way. We have summarized the derivations of these models studied to date in Table 1. All the derivations verify that a contact angle is determined at the triple line regardless of the external fields. Experiments also confirmed these findings [13-15]. Here, we will introduce the derivations by energy minimization using simple mathematics or calculus of variations.

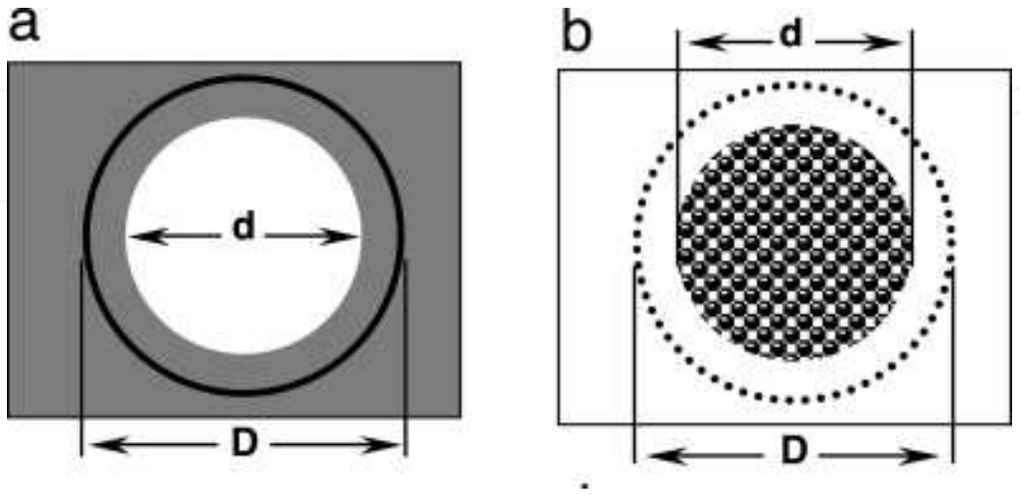

Figure 1. Depictions of (a) a hydrophilic spot on a hydrophobic surface and (b) a superhydrophobic spot on a smooth hydrophobic surface. Reprinted with permission from reference [7]. Copyright (2007) American Chemical Society.

Derivation method	External field	Region to determine a contact angle	Reference
Homogenization approach	N/A	At triple line	Xu and Wang, 2010 [16]
Fundamental calculus	N/A	At triple line	Seo et al., 2013 [17]
Fundamental calculus	N/A	At triple line	Whyman et al., 2008 [18]
Variational approach	Gravity	At triple line	Bormashenko, 2009 [19]
Variational approach	Electric field	At triple line	Bormashenko, 2012 [20]

Table 1. Derivations for the Wenzel model and the Cassie-Baxter model.

2. Derivation with simple mathematics

For the derivation of Young's equation in a rigorous way, the following assumptions will be used. First, the surface is ideal and it has no contact angle hysteresis. Thus, the contact line can freely move around. Second, the drop is in zero gravity and the shape of the drop is always a section of sphere, i.e., spherical cap.

As shown in Fig. 2, when the shape of the drop is deformed by spreading or contracting, the solid/liquid interfacial area varies with a contact angle that is a one-to-one function of the interfacial area. By the free movement of the contact line on an ideal surface, the drop can change freely its shape in order to satisfy the minimum energy state of the system. When the drop is at the equilibrium state, there will be no residual force at the contact line. At this point, the contact line and the shape of the drop will be fixed.

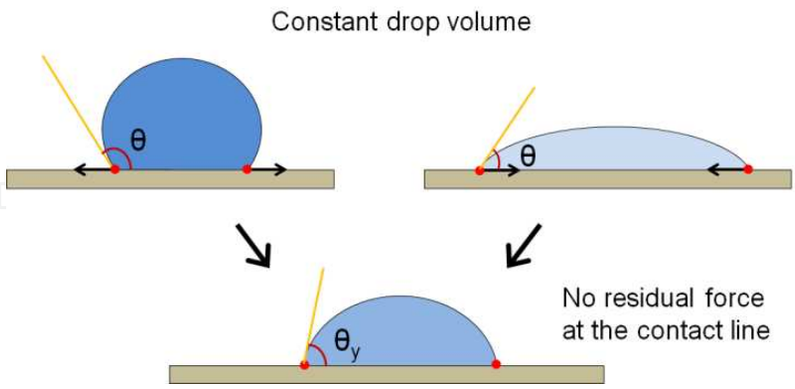

Figure 2. Formation of the contact angle of a drop on an ideal surface. Reprinted with permission from reference [17]. Copyright (2013) Springer-Verlag.

2.1. Derivation of Young's equation

With a thermodynamic approach, Young's equation can be derived with simple mathematics. Fig. 3 shows a drop on an ideal surface. The volume of the spherical cap is $V = \frac{\pi h}{6}(3r^2 + h^2)$ or

http://dx.doi.org/10.5772/61066

$V=\frac{\pi R^3}{3}(1-\cos\theta)^2(2+\cos\theta)$. The surface area of the cap is $A=2\pi Rh$ or $A=2\pi R^2(1-\cos\theta)$. The total energy of the system can be written as

$$E=\pi r^2\left(\gamma_{sl}-\gamma_{so}\right)+2\pi Rh\cdot\gamma=\pi(R\sin\theta)^2\left(\gamma_{sl}-\gamma_{so}\right)+2\pi R^2\left(1-\cos\theta\right)\gamma \tag{4}$$

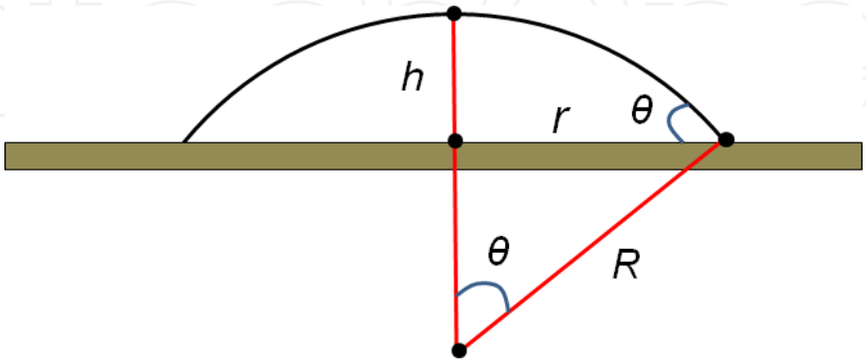

Figure 3. Cross-section of the drop on an ideal surface. Reprinted with permission from reference [17]. Copyright (2013) Springer-Verlag.

The variation of the energy is written as

$$dE=2\pi R\cdot\left[\left(\gamma_{sl}-\gamma_{so}\right)\cdot\left(\sin^2\theta dR+R\sin\theta\cos\theta d\theta\right)+\gamma\cdot\left(2\left(1-\cos\theta\right)dR+R\sin\theta d\theta\right)\right] \tag{5}$$

The variation of the energy is equal to zero at the equilibrium state ($dE=0$). Dividing both sides by dR is written as

$$\frac{dE}{dR}=2\pi R\cdot\left[\left(\gamma_{sl}-\gamma_{so}\right)\cdot\left(\sin^2\theta+R\sin\theta\cos\theta\frac{d\theta}{dR}\right)+\gamma\cdot\left(2\left(1-\cos\theta\right)+R\sin\theta\frac{d\theta}{dR}\right)\right]=0 \tag{6}$$

$\frac{dE}{dR}=0$ means that there is no energy variation by an infinitesimal change of the shape of the drop. At this point, the shape of the drop satisfies the minimum energy state. Here, in order to induce $\frac{d\theta}{dR}$, the constant-volume condition of the drop is used ($dV=0$).

The volume of the drop is given by

$$V=\frac{\pi R^3}{3}\left(1-\cos\theta\right)^2\left(2+\cos\theta\right) \tag{7}$$

$\frac{d\theta}{dR}$ can be obtained from the condition of the constant volume.

$$\frac{d\theta}{dR} = -\frac{(1-\cos\theta)(2+\cos\theta)}{R\sin\theta(1+\cos\theta)} \tag{8}$$

Substituting Eq. (8) into Eq. (6) gives

$$\begin{aligned}(\gamma_{sl}-\gamma_{so})\cdot\left(\sin^2\theta+\cos\theta\left(-\frac{(1-\cos\theta)(2+\cos\theta)}{(1+\cos\theta)}\right)\right)\\ +\gamma\cdot\left(2(1-\cos\theta)-\frac{(1-\cos\theta)(2+\cos\theta)}{(1+\cos\theta)}\right)=0\end{aligned} \tag{9}$$

Rearranging the above equation gives rise to the Young's equation.

$$\gamma_{sl}+\gamma\cos\theta = \gamma_{so} \tag{10}$$

2.2. Derivation of the Wenzel equation

Fig. 4 shows a drop in the Wenzel state. The radius of the drop is *a*. The radius of the smooth region of the substrate under the drop is *b*. When *b* is equal to zero, the substrate becomes a uniform rough surface. The contact line of the drop is assumed to be located on the rough region of the substrate.

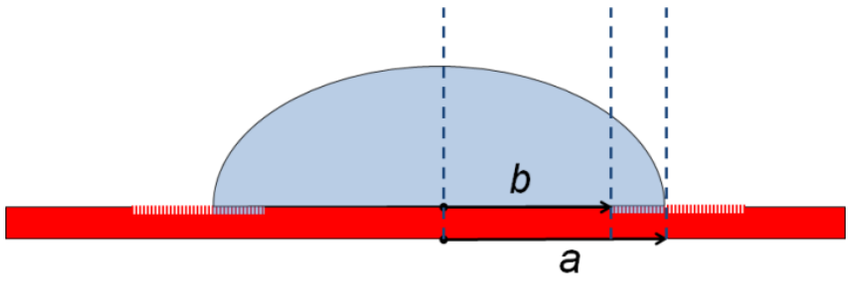

Figure 4. Schematic of the drop in the Wenzel state. The radius of the drop is *a*. The smooth region is *b*. Reprinted with permission from reference [17]. Copyright (2013) Springer-Verlag.

From the figure, the total energy of the system can be written as

$$E = \pi b^2(\gamma_{sl}-\gamma_{so}) + K\pi(a^2-b^2)(\gamma_{sl}-\gamma_{so}) + A_s\gamma \tag{11}$$

K is the surface roughness factor. A_s is the gas/liquid interfacial area. The variation of the energy is written as

$$dE = \mathrm{d}\left[\pi b^2(\gamma_{sl}-\gamma_{so})\right] + d\left[K\pi(a^2-b^2)(\gamma_{sl}-\gamma_{so})\right] + d\left[A_s\gamma\right] \tag{12}$$

http://dx.doi.org/10.5772/61066

Rearranging above equation, it will be written as

$$dE = K\pi\left(\gamma_{sl} - \gamma_{so}\right)d\left[a^2\right] + \gamma d\left[A_s\right] \tag{13}$$

It should be noted that the terms related to b^2 were eliminated because they are constant. Thus, the internal surface inside the contact line does not affect the apparent contact angle. There is a significant difference with the previous Wenzel model where the internal surface is considered as an important factor. From $dE=0$ at equilibrium and Eq. (8), the revised Wenzel equation is derived:

$$K\cos\theta_Y = \cos\theta \tag{14}$$

where θ_Y is the equilibrium contact angle on a smooth surface and θ is the apparent contact angle.

In the revised Wenzel equation, the definition on the surface roughness factor is different with the previous one. The roughness factor r in the previous Wenzel model came from the total area under the drop. However, the roughness factor K in Eq. (14) should be obtained from local region near contact line.

2.3. Derivation of the Cassie-Baxter equation

Fig. 5 shows a drop on a composite substrate that consists of two kinds of ideal surfaces. The area fraction of the red region is f_1 and the yellow region is f_2.

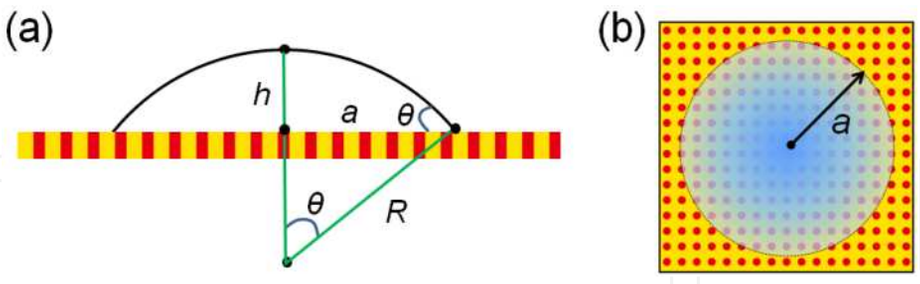

Figure 5. Schematic of the drop in the Cassie-Baxter state: (a) side-view, (b) top-view. Reprinted with permission from reference [17]. Copyright (2013) Springer-Verlag.

From the figure, the total energy of the system can be written as

$$E = f_1\pi a^2\left(\gamma_{sl,f_1} - \gamma_{so,f_1}\right) + f_2\pi a^2\left(\gamma_{sl,f_2} - \gamma_{so,f_2}\right) + A_s\gamma \tag{15}$$

Here, A_s is the gas/liquid interfacial area. The variation of the energy is written as

$$dE = C_1 d(R^2 \sin^2\theta) + C_2 d(R^2(1-\cos\theta)) \tag{16}$$

Here, $C_1 = f_1\pi(\gamma_{sl,f_1} - \gamma_{so,f_1}) + f_2\pi(\gamma_{sl,f_2} - \gamma_{so,f_2})$, $C_2 = 2\pi\gamma$

From *dE=0* at equilibrium and Eq. (8), the revised Cassie-Baxter equation is derived

$$f_1 \cos\theta_1 + f_2 \cos\theta_2 = \cos\theta \tag{17}$$

Assuming f_2 to be a fraction for contacting with air and $\theta_2 = \pi$, the revised Cassie-Baxter equation can be derived from Eq. (17). There is an important difference in the previous Cassie-Baxter equation and the revised one. The definition on the surface fraction is different. While it came from the total area under the drop in the previous model, the surface fraction in Eq. (17) should be obtained from the local region near the contact line. From the derivation, it can be also deduced that the property or the state of internal surface inside the triple line does not affect the apparent contact angle.

3. Derivation with calculus of variations

In the previous chapter, an external field, such as gravity, was not considered for simple derivation and it was possible to deal with the shape of the drop as a part of sphere. In this chapter, variational approach is employed and the shape of the drop can be distorted by the external field. Bormashenko used this approach for the first time to derive and develop the contact angle models [19]. To understand the variational approach, fundamental formulas in calculus of variations will be introduced briefly [21].

3.1. Calculus of variations

The basic concept of variational method is searching a function that has an extreme value (maximum or minimum) of a physical quantity, such as energy, length, area, time, and so on. In mathematical expression, objective function *J[y]* can be defined as

$$J[y] = \int_{x_0}^{x_1} F[x, y(x), y'(x), y''(x), \ldots]\, dx \tag{18}$$

Thus, the goal is to find function '*y*' that makes *J[y]* have an extreme value among countless number of *y* within the scope of the definite integral of a function [21].

With the variational method, we can solve many problems involving the determination of maxima or minima of functionals, such as the shortest smooth curve joining two distinct points in the plane [21], the shape of solid of revolution moving in a flow of gas with least resistance

http://dx.doi.org/10.5772/61066

[22], the plane curve down that a particle will slide without friction from one point to the other point in the shortest time [23], the curve passing through two given points to have minimum surface area by the rotation of the curve [21], and the shape of the flexible cable of given length suspended between two poles [24].

All of the above examples involve funtionals that can be written in the form,

$$J\left[y\right]=\int_{a}^{b}F\left[x,\ y\left(x\right),\ y'\left(x\right)\right]\ dx \tag{19}$$

There is a fundamental formula for solving the simple variational problems. This is the so-called Euler equation,

$$F_{y}-\frac{d}{dx}F_{y'}=0 \tag{20}$$

When a curve passes through two fixed end points, $y(a)=A$ and $y(b)=B$, the values of the arbitrary constants are simply determined by the end points.

However, as shown in Fig. 6, when both end points of the curve are always placed on $y=m(x)$ and $y=n(x)$, the transversality condition is an additional constraint that must be satisfied at the endpoints of the curve in order for $J[y]$ to have an extreme value. When the equation has following form,

$$J\left[y\right]=\int_{x_0}^{x_1}F\left[x,\ y\left(x\right),\ y'\left(x\right)\right]\ dx \tag{21}$$

the transversality condition is as follows:

$$\left[F+\left(m'-y'\right)F_{y'}\right]\Big|_{x=x_0}=0,\left[F+\left(n'-y'\right)F_{y'}\right]\Big|_{x=x_1}=0 \tag{22}$$

It is possible to obtain the curve that must simultaneously satisfy certain constraints as a subsidiary condition. When the form of a functional is the same as $J[y]=\int_{a}^{b}F[x,\ \ y(x),\ \ y'(x)]\ dx$, and the curve '$y$' should also satisfy the following constraint, $C=\int_{a}^{b}G[x,\ \ y(x),\ \ y'(x)]\ dx$, where C is constant, the curve 'y' that makes $J[y]$ a extreme value, satisfying the constraints, is a curve that makes the following $Q[y]$ an extreme value

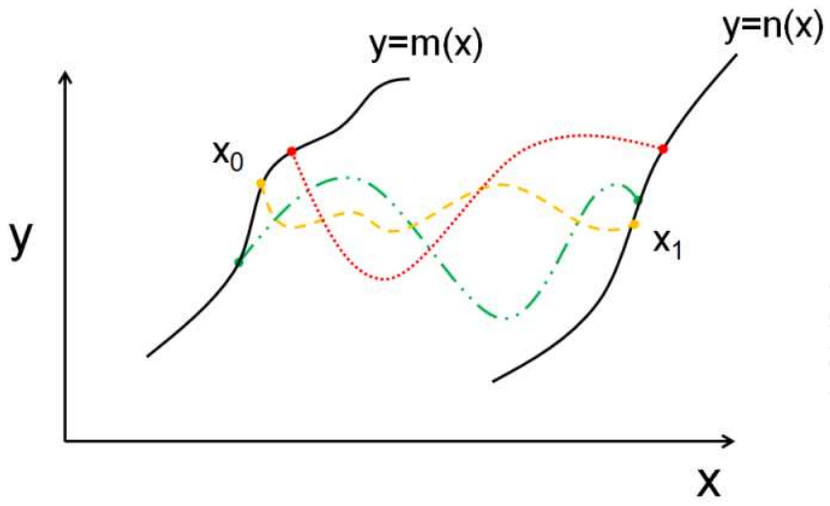

Figure 6. a) Transversality condition as additional constraints at the end points of the curve to have an extreme value required in the system.

$$Q[y] = \int_a^b (F + \lambda G)\, dx, \tag{23}$$

where λ is the Lagrange multiplier to be deduced from the subsidiary condition.

Therefore, the curve 'y' should satisfy the following equation:

$$F_y - \frac{d}{dx}F_{y'} + \lambda\left(G_y - \frac{d}{dx}G_{y'}\right) = 0. \tag{24}$$

These fundamental equations will be used to derive the contact angle models. How a drop takes its contact angle can be understood more clearly from the variational approach.

3.2. Derivation of Young's equation

Fig. 7 shows a drop on an ideal surface in a three-dimensional (3D) system. The symmetrical 3D drop sitting on the surface subject to energy density $U(r,\ h(r))$, due to an external field such as gravity, is considered. The free energy for the drop, $G(h,\ h',\ r)$, is given by the integral.

$$G(h,\ h',\ r) = \int_0^a \left[2\pi r\gamma \cdot \sqrt{1 + \left(\frac{dh}{dr}\right)^2} + U(r,h) + \left[2\pi r\left(\gamma_{SL} - \gamma_{SO}\right)\right]\right] dr \tag{25}$$

http://dx.doi.org/10.5772/61066

The linear density $U(r,\ h(r))$ of the additional energy with the dimension of (J m^{-1}) is defined by the expression, $U(r,\ h(r))=\int_0^{h(r)} 2\pi r w(r,\ y)dy$, where $w(r,\ y)$ is the volume energy density of the drop in the external field (J m^{-3}), $h(r)$ is the local height of the liquid surface, and h' is $\frac{dh}{dr}$.

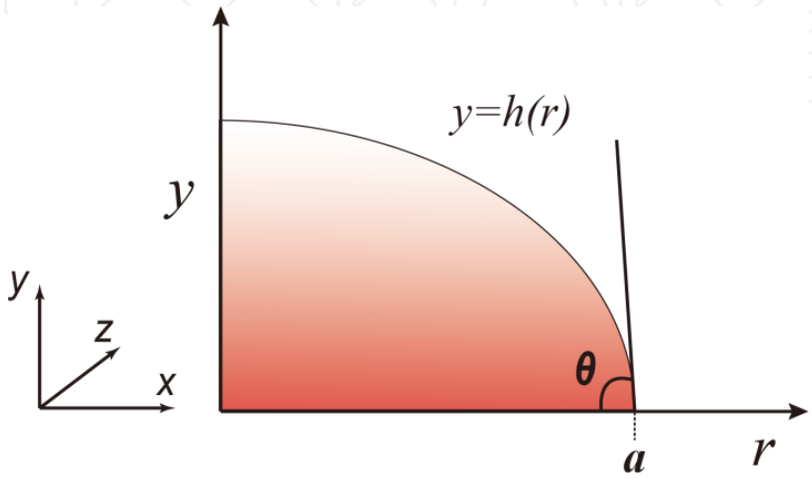

Figure 7. The cross-section of the drop deposited on an ideal surface.

The constant volume V_0 of a drop is assumed as a subsidiary condition.

$$V_0 = \int_0^a 2\pi r \cdot \left[h(r)\right]dr \tag{26}$$

From Eq. (25) and Eq. (26), the problem of energy minimization in the total system is reduced to the one of minimization of the following functional:

$$G = \int_0^a \left[\tilde{G}(h,h',\ r)\right]dr \tag{27}$$

where,

$$\tilde{G}(h,h',r) = 2\pi\gamma r\sqrt{1+h'^2} + U(r,h) + 2\pi r(\gamma_{SL} - \gamma_{SO}) + 2\pi\beta rh \tag{28}$$

and β is the Lagrange multiplier to be deduced from Eq. (26). Transversality condition is the one that should be satisfied at the end points in order to minimize the total energy of the system. The transversality condition at the end point a is written as

$$\left[\tilde{G} - h'\tilde{G}_{h'}\right]_{r=a} = 0 \tag{29}$$

where $\tilde{G}_{h'}$ denotes $\frac{\partial \tilde{G}}{\partial h'}$. Considering $h(a)=0$ and $U(a,\ h(a))=0$, substitution of Eq. (28) into the transversality condition gives

$$\left[\gamma \cdot \sqrt{1+h'^2} + \left(\gamma_{SL} - \gamma_{SO}\right) - h' \cdot \left[\frac{\gamma \cdot h'}{\sqrt{1+h'^2}}\right]\right]_{r=a} = 0 \tag{30}$$

Rearranging Eq. (30) gives

$$\gamma \cdot \left(\frac{1}{\sqrt{1+h'^2}}\right) + \left(\gamma_{SL} - \gamma_{SO}\right) = 0 \tag{31}$$

Taking into account $h' = \tan(\pi - \theta) = -\tan\theta$ at the triple line in Fig. 7, Eq. (31) is rewritten as

$$\gamma \cdot \left(\frac{1}{\sqrt{1+\tan^2\theta}}\right) + \left(\gamma_{SL} - \gamma_{SO}\right) = 0 \tag{32}$$

Rearrangement of Eq. (32) gives Young's equation:

$$\cos\theta = \frac{\gamma_{SO} - \gamma_{SL}}{\gamma} \tag{33}$$

where the apparent contact angle, θ, is the equilibrium contact angle (θ_Y).

Young's equation was derived from the transversality condition. It means that the equilibrium contact angle (Young's equation) must be satisfied at the contact line in order to minimize the total energy of the system. The variational approach assures that the contact angle is determined at the contact line. It should be noted that the external field, such as gravity, cannot affect the equilibrium contact angle, although it distorts the shape of the drop.

3.3. Derivation of the Wenzel equation

Fig. 8 shows a symmetrical 3D drop in the Wenzel state. The drop is placed on a rough surface with full contact with the solid surface (no air gap). *K* is a surface roughness factor that is defined as the ratio of the actual area to the projected area of the substrate. The radius of the drop is *a*. The smooth region under the drop is *b*. The contact line of the drop is assumed to be

http://dx.doi.org/10.5772/61066

located on the rough region of the surface. The free energy for the drop, $J(h,\ h',\ r)$, is given by the integral

$$J(h,\ h',\ r)=\int_0^a\left[2\pi r\gamma\cdot\sqrt{1+\left(\frac{dh}{dr}\right)^2}+U(r,h)\right]dr+ \\ +\pi b^2(\gamma_{SL}-\gamma_{SO})+K\int_b^a\left[2\pi r(\gamma_{SL}-\gamma_{SO})\right]dr \tag{34}$$

The above equation can be rearranged as

$$J(h,\ h',\ r)=\int_0^a\left[2\pi r\gamma\cdot\sqrt{1+\left(\frac{dh}{dr}\right)^2}+U(r,h)\right]dr+K\int_b^a\left[2\pi r(\gamma_{SL}-\gamma_{SO})\right]dr+ \\ +K\int_0^b\left[2\pi r(\gamma_{SL}-\gamma_{SO})\right]dr-K\int_0^b\left[2\pi r(\gamma_{SL}-\gamma_{SO})\right]dr+\pi b^2(\gamma_{SL}-\gamma_{SO}) \tag{35}$$

where the last two terms are constants, giving

$$C=(1-K)\pi b^2(\gamma_{SL}-\gamma_{SO}) \tag{36}$$

Here, since the contact angle is independent of the absolute value of the total energy, the constant energy term has no effect on the contact angle [17]. Thus, the free energy can be redefined as follows:

$$G(h,\ h',\ r)=J(h,\ h',r)-C=\int_0^a\left[2\pi r\gamma\cdot\sqrt{1+\left(\frac{dh}{dr}\right)^2}+U(r,h)+2\pi rK(\gamma_{SL}-\gamma_{SO})\right]dr \tag{37}$$

Now, considering the constant volume of a drop as a subsidiary condition and the transversality condition, the revised Wenzel equation is derived:

$$\cos\theta=K\frac{\gamma_{SO}-\gamma_{SL}}{\gamma}=K\cos\theta_Y \tag{38}$$

where θ_Y is the equilibrium contact angle on a smooth solid surface and θ is an apparent contact angle.

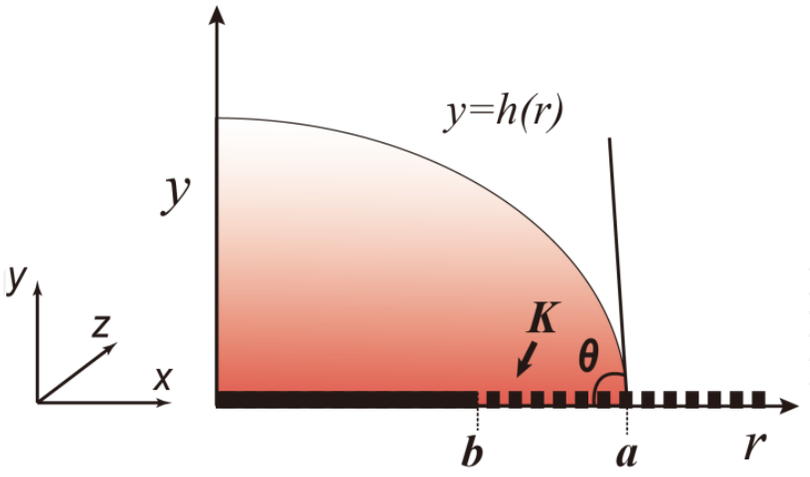

Figure 8. The cross-section of the drop placed on a rough surface.

3.4. Derivation of the Cassie-Baxter equation

Fig. 9 shows a symmetrical 3D drop in the Cassie-Baxter state. The drop is placed on a composite surface consisting of two surfaces. The radius of the drop is a. The free energy for the drop, $G(h,\ h',\ r)$, is given by the integral

$$G(h,\ h',\ r)=\int_0^a\left[2\pi r\gamma\cdot\sqrt{1+\left(\frac{dh}{dr}\right)^2}+U(r,h)\right]dr+ \\ +f_1\int_0^a\left[2\pi r\left(\gamma_{SL}^1-\gamma_{SO}^1\right)\right]dr+f_2\int_0^a\left[2\pi r\left(\gamma_{SL}^2-\gamma_{SO}^2\right)\right]dr \tag{39}$$

where f_1 and f_2 are area fractions of surface 1 and surface 2, respectively. The above equation can be rearranged as

$$G(h,\ h',\ r)=\int_0^a\left[2\pi r\gamma\cdot\sqrt{1+\left(\frac{dh}{dr}\right)^2}+U(r,h)+f_1\left[2\pi r\left(\gamma_{SL}^1-\gamma_{SO}^1\right)\right]+f_2\left[2\pi r\left(\gamma_{SL}^2-\gamma_{SO}^2\right)\right]\right]dr \tag{40}$$

Now, considering the constant volume of a drop as a subsidiary condition and the transversality condition, the revised Cassie-Baxter equation is derived.

$$\cos\theta=f_1\frac{\gamma_{SO}^1-\gamma_{SL}^1}{\gamma}+f_2\frac{\gamma_{SO}^2-\gamma_{SL}^2}{\gamma}=f_1\cos\theta_Y^1+f_2\cos\theta_Y^2 \tag{41}$$

http://dx.doi.org/10.5772/61066

where θ_Y^1 and θ_Y^2 are the equilibrium contact angles on the surface 1 and the surface 2. θ is an apparent contact angle.

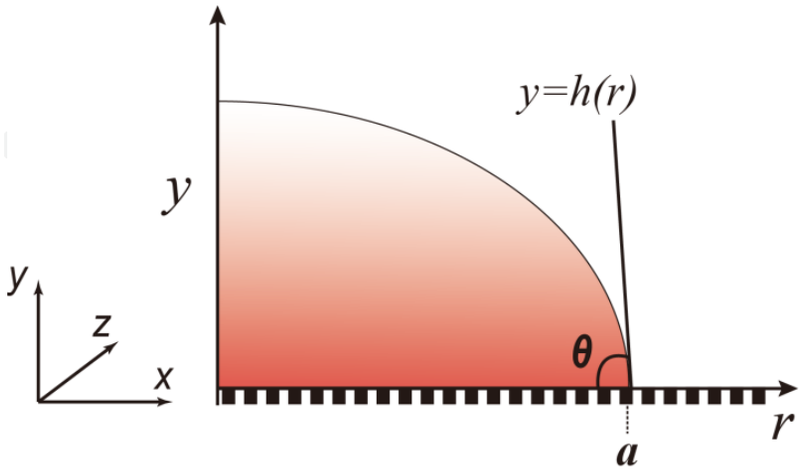

Figure 9. The cross-section of the drop deposited on a composite surface.

Likewise, a general Cassie-Baxter equation for different composite surfaces can be derived [25]. In the revised equation (Eq. (41)), the area fractions are related to only the local region at the contact line.

3.5. Contact angles under other conditions

By employing the variational approach, it is easy to understand the behavior of the contact angles under various conditions. As mentioned above, after obtaining the total energy of the system under each condition, the contact angles are obtained from the transversality condition. In this way, the contact angles of the drops on a gradient surface [19], a rotating surface [26], a curved surface [25], and a surface with an electric field [20] were studied. To conclude, it was demonstrated that if the factors or conditions to be considered do not affect the surface energy and the surface topography near the contact line, they cannot affect the contact angles.

4. Discussion

The contact angle of a drop was considered from a thermodynamic point of view. The contact angle models (Young's equation, Wenzel equation, and Cassie-Baxter equation) were re-derived by the energy minimization and the variational approach. It was clearly demonstrated from the derivations that the contact angle of a drop is a necessary condition that must be satisfied at the contact line in order to minimize the total energy of the system. In other words, a drop takes an optimal contact angle to have the lowest energy of the system. When the optimal contact angle is not satisfied, the total energy of the system is not at a local minimum. Thus, residual force exists at the contact line and changes the shape of the drop until it disappears, as shown in Fig. 2.

Two important points can be deduced from the derivations [19, 27]. Firstly, the contact angle is determined by the infinitesimal region at the contact line. The internal surface inside the contact line does not affect the contact angle. Thus, the roughness factor in the Wenzel equation or the area fraction in the Cassie-Baxter equation should be defined in the contact line region. Secondly, the contact angle is independent of the external factors that do not affect the surface energy. Fig. 10 shows the behavior of the contact angle on an ideal surface under various conditions. The contact angle is not affected by pressure, drop size, gravity, curvature of substrate, rotation of the substrate, and existence of a needle or defects.

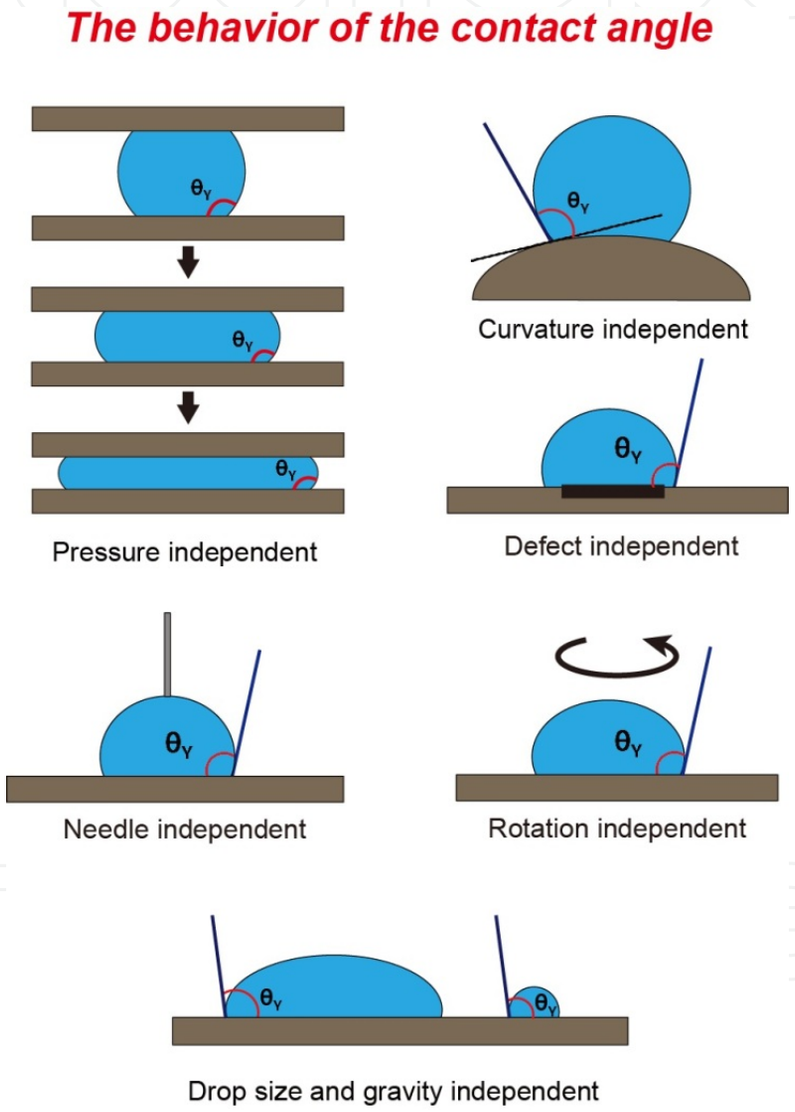

Figure 10. The behavior of the contact angle on an ideal surface under various conditions.

During the derivations, it has been assumed that the contact line moves freely on the surfaces and there is no contact angle hysteresis. However, all of real surfaces are not ideal and have contact angle hysteresis [28]. The contact line cannot move freely on them. The surfaces have a range of static contact angles between two extreme values of an advancing angle and a

http://dx.doi.org/10.5772/61066

receding angle [29]. So, the real surfaces are hard to describe with a single equation, while Young's equation, the Wenzel equation, or the Cassie-Baxter equation yield a single contact angle. Especially, when a drop on a rough surface takes the Wenzel state, the contact angle hysteresis is very large violating the assumption of the free movement of the contact line [30, 31] and a specific static contact angle is hardly meaningful to describe the surface [32, 33]. Whereas a superhydrophobic surface has a very low contact angle hysteresis having a narrow range of static contact angles. A drop on the surface takes the Cassie-Baxter state. The contact line can easily move on it. Thus, the superhydrophobic surface can be considered as pseudo-ideal surface from the theoretical viewpoint in that the contact line can move freely. For this reason, the Cassie-Baxter equation has been widely used for the superhydrophobic surface.

In using the contact angle equations, careful attention is required. When the length scale of the pattern in the surface roughness is smaller than an order of a micrometer, additional correction factors should be considered including line tension and disjoining pressure [34-36]. However, the contact angle models do not contain these factors. In addition, they do not consider the shape and size of the pattern, which actually affect the contact angle [37]. Therefore, these equations should be used with caution and more advanced equations should be developed in order to describe the contact angle on the real surface.

5. Conclusion

Young's equation, the Wenzel equation, and the Cassie-Baxter equations were re-derived from a thermodynamic point of view. From the derivations, the behavior of the contact angle could be deduced. In an ideal situation, the contact angle is determined by the infinitesimal region in the vicinity of contact line, not by the internal surface inside the contact line. The contact angle is also independent of the external factors that do not affect the surface energy. Thus, it is not affected by pressure, drop size, gravity, curvature of the substrate surface, rotation of the substrate, and existence of a needle or defects. It was explained from the view point of the contact angle hysteresis why these equations are not proper to describe the real common surfaces although the Cassie-Baxter equation has been widely used for a superhydrophobic surface. Also, the limitations of the equations were discussed. It is expected that this study will provide a deeper understanding of the validity of the contact angle models and the nature of the contact angle.

Author details

Kwangseok Seo, Minyoung Kim and Do Hyun Kim*

*Address all correspondence to: dohyun.kim@kaist.ac.kr

Department of Chemical and Biomolecular Engineering, Korea Advanced Institute of Science and Technology, Daejeon, South Korea

References

[1] Wenzel, R.N. (1936). Resistance of Solid Surfaces to Wetting by Water. *Industrial & Engineering Chemistry,* vol. 28, pp. 988-994, ISSN 0888-5885.

[2] Cassie, A.B.D. & Baxter, S. (1944). Wettability of Porous Surfaces. *Transactions of the Faraday Society,* vol. 40, pp. 546-551, ISSN 0014-7672.

[3] Xu, W., Shi X. & Lu S. (2011). Controlled Growth of Superhydrophobic Films without any Low-Surface-Energy Modification by Chemical Displacement on Zinc Substrates. *Materials Chemistry and Physics*, vol. 129, pp. 1042-1046, ISSN 0254 0584.

[4] Tuteja, A., Choi, W., Ma, M., Mabry, J.M., Mazzella, S.A., Rutledge, G.C., McKinley, G.H. & Cohen, R.E. (2007). Designing Superoleophobic Surfaces. *Science*, vol. 318, pp. 1618-1622, ISSN 1095-9203.

[5] Noh, J., Lee, J.-H., Na, S., Lim, H. & Jung, D.-H. (2010). Fabrication of Hierarchically Micro- and Nano-structured Mold Surfaces Using Laser Ablation for Mass Production of Superhydrophobic Surfaces. *Japanese Journal of Applied Physics*, vol. 49, 106502, ISSN 1347-4065.

[6] Wang, C., Yao, T., Wu, J., Ma, C., Fan, Z., Wang, Z., Cheng, Y., Lin, Q. & Yang, B. (2009). Facile Approach in Fabricating Superhydrophobic and Superoleophilic Surface for Water and Oil Mixture Separation, *ACS Applied Materials & Interfaces*, vol. 1, pp. 2613-2617, ISSN 1944-8252.

[7] Gao, L. & McCarthy, T.J. (2007). How Wenzel and Cassie were Wrong. *Langmuir*, vol. 23, pp. 3762-3765, ISSN 1520-5827.

[8] McHale, G. (2007). Cassie and Wenzel: Were They Really So Wrong? *Langmuir,* vol. 23, pp. 8200-8205, ISSN 1520-5827.

[9] Panchagnula, M.V. & Vedantam, S. (2007). Comment on How Wenzel and Cassie Were Wrong by Gao and McCarthy. *Langmuir*, vol. 23, pp. 13242, ISSN 1520-5827.

[10] Nosonovsky, M. (2007). On the Range of Applicability of the Wenzel and Cassie Equations. *Langmuir*, vol. 23, pp. 9919-9920, ISSN 1520-5827.

[11] Marmur, A. & Bittoun, E. (2009). When Wenzel and Cassie Are Right: Reconciling Local and Global Considerations. *Langmuir*, vol. 25, pp. 1277-1281, ISSN 1520-5827.

[12] Erbil, H.Y. (2014). The Debate on the Dependence of Apparent Contact Angles on Drop Contact Area or Three-Phase Contact Line: A Review. *Surface Science Reports*, vol. 69, pp. 325-365, ISSN 0167-5729.

[13] Choi, W., Tuteja, A., Mabry, J.M., Cohen, R.E. & McKinley, G.H. (2009). A Modified Cassie-Baxter Relationship to Explain Contact Angle Hysteresis and Anisotropy on non-Wetting Textured Surfaces. *Journal of Colloid and Interface Science*, vol. 339, pp. 208-216, ISSN 0021-9797.

[14] Seo, K., Kim, M., & Kim, D.H. (2014). Candle-Based Process for Creating a Stable superhydrophobic surface. *Carbon*, vol. 68, pp. 583-596, ISSN 0008-6223.

[15] ChangWei, Y., Feng, H. & PengFei, H. (2010). The Apparent Contact Angle of Water Droplet on the Micro-Structured Hydrophobic Surface. *Science China Chemistry*, vol. 53, pp. 912-916, ISSN 1869-1870.

[16] Xu, X. & Wang, X. (2010). Derivation of the Wenzel and Cassie Equations from a Phase Field Model for Two Phase Flow on Rough Surface. *SIAM Journal on Applied Mathematics*, vol. 70, pp. 2929-2941, ISSN 0036-1399.

[17] Seo, K., Kim, M., & Kim, D.H. (2013). Validity of the Equations for the Contact Angle on Real Surfaces. *Korea-Australia Rheology Journal*, vol. 25, pp.175-180, ISSN 2093-7660.

[18] Whyman, G., Bormashenko, E. & Stein, T. (2008). The Rigorous Derivation of Young, Cassie-Baxter and Wenzel Equations and the Analysis of the Contact Angle Hysteresis Phenomenon. *Chemical Physics Letters*, vol. 450, pp. 355-359, ISSN 0009-2614.

[19] Bormashenko, E. (2009). A Variational Approach to Wetting of Composite Surfaces: Is Wetting of Composite Surfaces a One-Dimensional or Two-Dimensional Phenomenon. *Langmuir*, vol. 25, pp. 10451-10454, ISSN 1520-5827.

[20] Bormashenko, E. (2012). Contact Angles of Sessile Droplets Deposited on Rough and Flat Surfaces in the Presence of External Fields. *Mathematical Modelling of Natural Phenomena*, vol. 7, pp. 1-5, ISSN 0973-5348.

[21] Gelfand, I.N. & Fomin, S.V. (2000). *Calculus of Variations*, Dover, ISBN-13: 978-0-486-41448-5; ISBN-10: 0-486-41448-5, New York.

[22] Eggers, A.J., Resnikoff, M.M., & Dennis, D.H. (1957). Bodies of Revolutions Having Minimum Drag at High Supersonic Air Speeds, NACA Report No. 1306.

[23] Filobello-Nino, U., Vazquaz-Leal, H., Pereyra-Diaz, D., Yildirim, A., Peres-Sesma, A., Castaneda-Sheissa, R., Sanchez-Orea, J. & Hoyos-Reyes, C. (2013) A Generalization of the Bernoulli's Method Applied to Brachistochrone-like Problems. *Applied Mathematics and Computation*, vol. 219, pp. 6707-6718, ISSN 0096-3003.

[24] Mareno, A. & English, L.Q. (2009). The Stability of the Catenary Shapes for a Hanging Cable of Unspecified Length. *European Journal of Physics*, vol. 30, pp. 97-108, ISSN 1361-6404.

[25] Bormashenko, E. (2009). Wetting of Flat and Rough Curved Surfaces. *The Journal of Physical Chemistry C*, vol. 113, pp. 17275-17277, ISSN 1932-7455.

[26] Bormashenko E. (2013). Contact Angles of Rotating Sessile Droplets. *Colloids and Surfaces A: Physicochemical and Engineering Aspects*, vol. 432 pp. 38-41, ISSN 0927-7757.

[27] Seo, K., Kim, M., & Kim, D.H. (2015). Effects of Drop Size and Measuring Condition on Static Contact Angle Measurement on a Superhydrophobic Surface with Goniometric Technique. *Korean Journal of Chemical Engineering*, in print, ISSN 1975-7220.

[28] Gleiche, M., Chi, L., Geding, E. & Fuchs, H., (2001). Anisotropic Contact-Angle Hysteresis of Chemically Nanostructured Surfaces. *Chem Phys Chem*, vol. 2, pp. 187-191, ISSN 1439-7641.

[29] Marmur, A. (2006). Soft Contact: Measurement and Interpretation of Contact Angles. *Soft Matter*, vol. 2. pp. 12-17, ISSN 1744-6848.

[30] Morra, M., Occhiello, E., & Garbassi, F. (1989). Contact Angle Hysteresis in Oxygen Plasma Treated Poly(tetrafluoroethylene). *Langmuir*, vol. 5, pp.872-876, ISSN 1520-5827.

[31] Cao, L. & Gao, D. (2010). Transparent Superhydrophobic and Highly Oleophobic Coatings. *Faraday Discussions*, vol. 146, pp. 57-65, ISSN 1359-6640.

[32] Gao, L. & McCarthy, T.J. (2006) Contact Angle Hysteresis Explained. *Langmuir*, vol. 22, pp. 6234-6237, ISSN 1520-5827.

[33] Gao, L. & McCarthy, T.J. (2009). Wetting 101°. *Langmuir*, vol. 25, pp. 14105-14115, ISSN 1520-5827.

[34] de Gennes, P.G., Brochard-Wyart, F., & Quéré, D. (2003). *Capillarity and Wetting Phenomena*, Springer, ISBN 0-387-00592-7, Berlin.

[35] Wong, T.-S. & Ho, C.-M. (2009). Dependence of Macroscopic Wetting on Nanoscopic Surface Textures. *Langmuir*, vol. 25, pp. 12851-12854, ISSN 1520-5827.

[36] Marmur, A. & Krasovitski, B. (2002). Line Tension on Curved Surfaces: Liquid Drops on Solid Micro- and Nanospheres. *Langmuir*, vol. 18, pp. 8919-8923, ISSN 1520-5827.

[37] Cansoy, C.F., Erbil, H.Y., Akar, O., & Akin, T. (2011). Effect of Pattern Size and Geometry on the Use of Cassie-Baxter Equation for Superhydrophobic Surfaces. *Colloids and Surfaces A: Physicochemic*al and Engineering Aspects, vol. 386, pp. 116-124, ISSN 0927-7757.